SUPPLEMENTAL MATERIAL

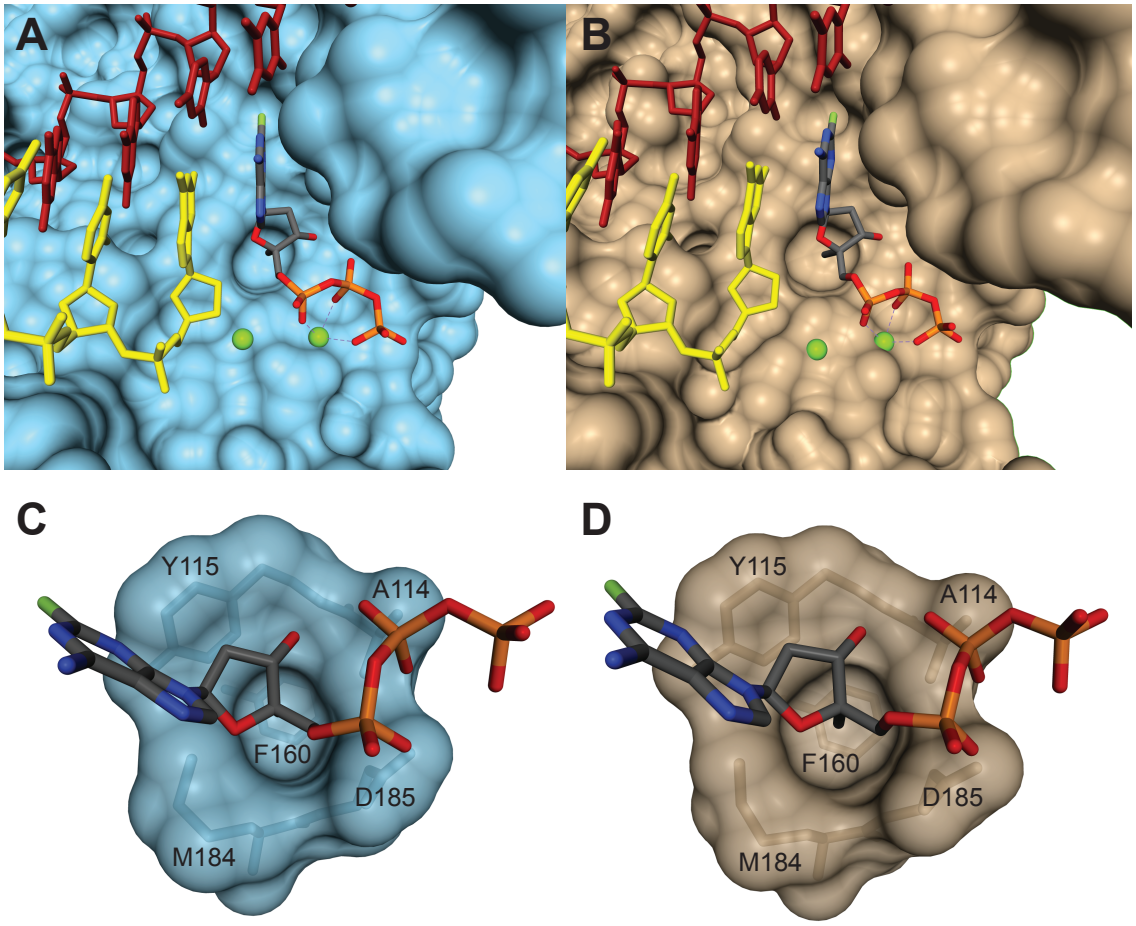

Figure S1. Positioning of MK-8591-TP in the polymerase active site of HIV-1 RT (A and C) and in a molecular model of the HIV-2 RT/inhibitor complex (B and D). In all four panels, the inhibitor is rendered in Corey-Pauling-Koltun–colored sticks and is shown as the incoming nucleotide substrate (i.e., the N-site complex). Catalytic magnesium ions are represented as green spheres. Template and nascent nucleic acid strands are shown in dark red and yellow, respectively. In panels A and C, portions of the fingers and palm subdomains of RT have been omitted to obtain an unobstructed view of the active site. Atomic coordinates for the HIV-1 RT structure

are from Protein Data Bank file 5J2M (1). The structure shown in panels B and D was generated by homology modeling (using 5JM2 as the reference structure) as previously described (2) and was energy minimized using the YASARA force field (www.yasara.org/minimizationserver.htm) (3). All illustrations were generated in UCSF Chimera (version 1.11.2; University of California, San Francisco, CA) (4).

References

1. **Salie ZL, Kirby KA, Michailidis E, Marchand B, Singh K, Rohan LC, Kodama EN, Mitsuya H, Parniak MA, Sarafianos SG.** 2016. Structural basis of HIV inhibition by translocation-defective RT inhibitor 4'-ethynyl-2-fluoro-2'-deoxyadenosine (EFdA). Proc Natl Acad Sci U S A **113:**9274-9279.
2. **Smith RA, Raugi DN, Wu VH, Leong SS, Parker KM, Oakes MK, Sow PS, Ba S, Seydi M, Gottlieb GS, University of Washington-Dakar HIVSG.** 2015. The nucleoside analog BMS-986001 shows greater in vitro activity against HIV-2 than against HIV-1. Antimicrob Agents Chemother **59:**7437-7446.
3. **Krieger E, Joo K, Lee J, Lee J, Raman S, Thompson J, Tyka M, Baker D, Karplus K.** 2009. Improving physical realism, stereochemistry, and side-chain accuracy in homology modeling: Four approaches that performed well in CASP8. Proteins **77 Suppl 9:**114-122.
4. **Pettersen EF, Goddard TD, Huang CC, Couch GS, Greenblatt DM, Meng EC, Ferrin TE.** 2004. UCSF Chimera--a visualization system for exploratory research and analysis. J Comput Chem **25:**1605-1612.

Table S1. Susceptibility of HIV-1_{NL4-3} and HIV-2_{ROD9} to additional ARV drugs.

	EC_{50} (nM)[a]			
HIV clone[b]	Raltegravir	d4T	AZT	TDF
HIV-1_{NL4-3}	11 ± 1.4 (5)	800 ± 300 (5)	29 ± 11 (2)	13 ± 1.3 (3)
HIV-2_{ROD9}	13 ± 7.2 (7)	800 ± 470 (4)	28 ± 3.2 (2)	6.4 ± 1.3 (4)

[a] EC_{50}, 50% effective concentration in the MAGIC-5A single-cycle assay. Values are means ± standard deviations. Values in parentheses indicate the number of independent dose-response assays performed for each inhibitor. Abbreviations are as follows: d4T, stavudine; AZT, zidovudine; TDF, tenofovir disoproxil fumarate.

[b] Viruses produced from full-length plasmids pNL4-3 and pROD9.

Table S2. Susceptibilities of HIV-2 RT mutants to raltegravir.

HIV clone[a]	Genotype[b]	EC_{50} (nM)[c]	n[d]	Fold change[e]
HIV-2_{ROD9}	wild-type	13 ± 7.2	7	
	K65R	12 ± 1.4	3	0.9
	M184V	9.7 ± 4.7	3	0.7
	K65R+Q151M	8.2 ± 2.5	3	0.6
	Q151M+M184V	16 ± 1.9	3	1.2
	K65R+Q151M+M184V	15 ± 6.6	4	1.2
	K65R+K70R+Q151M+M184V	12 ± 3.8	3	0.9
	K65R+Y115F+Q151M+M184V	16 ± 8.9	4	1.2
HIV-$2_{ROD9\text{-}4.7a}$	K65R+N69S+V111I+Q151M+M184V	15 ± 1.5	3	1.2

[a] Viruses produced from full-length plasmids pROD9, and patient-derived clone pROD9-4.7a.

[b] Amino acid changes listed for HIV-2_{ROD9} were engineered by site-directed mutagenesis. Changes listed for HIV-$2_{ROD9\text{-}4.7a}$ were encoded by a *pol* gene segment that was PCR-amplified from an HIV-2–infected patient (see text for details).

[c] EC_{50}, 50% effective concentrations measured in the MAGIC-5A single-cycle assay. Values are means ± standard deviations.

[d] Number of independent dose-response assays performed for each strain.

[e] EC_{50} for the mutant divided by the EC_{50} for wild-type HIV-2_{ROD9}.